Reply to comment by K. Pedoja et al. on "Tectonic record of strain buildup and abrupt coseismic stress release across the northwestern Peru coastal plain, shelf, and continental slope during the past 200 kyr"

Jacques Bourgois, Didier Bourles, Regis Braucher

Reply to comment by K. Pedoja et al. on "Tectonic record of strain buildup and abrupt coseismic stress release across the northwestern Peru coastal plain, shelf, and continental slope during the past 200 kyr"

Jacques Bourgois,[1] Didier Bourles,[2] and Régis Braucher[2]

Received 10 June 2011; revised 4 July 2011; accepted 25 July 2011; published 10 September 2011.

Citation: Bourgois, J., D. Bourles, and R. Braucher (2011), Reply to comment by K. Pedoja et al. on "Tectonic record of strain buildup and abrupt coseismic stress release across the northwestern Peru coastal plain, shelf, and continental slope during the past 200 kyr", *J. Geophys. Res.*, *116*, B09402, doi:10.1029/2011JB008582.

1. Introduction

[1] We thank the authors of the comment on "Tectonic record of strain buildup and abrupt coseismic stress release across the northwestern Peru coastal plain, shelf, and continental slope during the past 200 kyr", to give us a further opportunity to better discuss our data and hypotheses on the structure and evolution of this portion of the Andes forearc. This Reply consists of a detailed response to each comment raised by Pedoja and coauthors in order to clarify any doubt and to have a more effective and pertinent discussion. Because the paper by *Bourgois et al.* [2007] was published four years ago, this reply allows us to update several fundamental aspects including the coastal landform origin, the El Niño rainfall characteristics, the ^{10}Be data, the shoreline angle concept, and the Mancora Tablazo uplift rate.

2. Coastal Landform

[2] *Pedoja et al.* [2011] claim that the landforms described along the Cabo Blanco transect [*Bourgois et al.*, 2007, Figure 5, 6, and 9] are not breaking wave geomorphic features. From base to top these landforms, which exhibit a prominent staircase geomorphic signature (Figure 1) include: (1) a short seaward sloping platform covered by shingle or beach gravel, (2) a wave cut notch, which develops at the base of a cliff indicating breaking wave active erosion when formed, (3) a subvertical cliff associated with rockfalls, and (4) a cap of casehardened sandstone [*Sunamura*, 1992]. In addition to the geomorphic evidence stated in the original paper by *Bourgois et al.* [2007], the following basic points (Figure 1) validate the previous report: (1) The staircase geomorphic features extend along the coastal fringe, from the Present coastline to within 500 m landward at less than 100 m elevation. At this site, the cliffs are looking seaward. (2) Two faults of pre-Taime Formation age (i.e., older than 160 ± 12 ka) trending NE-SW bound the sampling area to the east and to the west. The Eocene sandstones exhibiting the staircase signature, outcrop along a local horst structure. Because the Eocene sandstones are more competent than rocks outcropping to the north and to the south, they are more prone to record and preserve the imprint of coastal landforms through time. Although, *Pedoja et al.* [2011] reject the coastal origin for the geomorphic markers, they identify no clear process (i.e., wind, and or meteoric water?) causing the staircase morphologic setup of the studied area. They just say: "we consider that these features formed above sea level by erosion of weaker strata…." We do note that breaking wave active erosion also attacks preferentially weaker strata in similar fashion as other processes of weathering. As proposed in the original work by *Bourgois et al.* [2007], the 16 raised coastal regressive terraces, which were carved during the past 21.2–26 kyr (Table 1) along the Cabo Blanco segment, are the signature of major repeated seismic events [*Plafker*, 1969; *Thatcher*, 1984]. These coastal regressive terraces provide direct information on the uplift history of the inboard major wave cut platform, the so-called Mancora Tablazo (see section 5).

3. El Niño Extreme Rainfall

[3] On the basis of grossly localized field pictures and fairly old literature [*Spruce*, 1864; *Carranza*, 1891; *Eguiguren*, 1894] *Pedoja et al.* [2011] claim that the area studied by *Bourgois et al.* [2007] is in a transitional climate zone, and has suffered strong erosion by heavy rainfall during El Niño events. Using rainfall data from 66 stations, *Goldberg et al.* [1987] provided contour maps describing the daily rainfall characteristics of northwestern Peru area during the 1982–1983 El Niño event. These data exhibit localized storms, which may then disperse over wider areas of the region during the following 2–3 days. The region located east of the Amotapes massif (i.e., 5°10′S- 80–17′W, east of Chulucanas) is the focal point for such extreme rainfall events [see *Goldberg et al.*, 1987, Figure 5]. *Takahashi* [2004] has shown that the rainfall events, which occurred on the Chulucanas area (located 55 km east of Piura) during the 2002 El Niño event tended to be clustered

[1]Institut des Sciences de la Terre, UMR 7193, CNRS, Université Pierre et Marie Curie, Paris, France.
[2]Centre Européen de Recherche et d'Enseignement des Geosciences de l'Environnement, UMR 6635, Europôle Méditerranéen de l'Arbois, Aix-Marseille Université, Aix-en-Provence, France.

0148-0227/11/2011JB008582

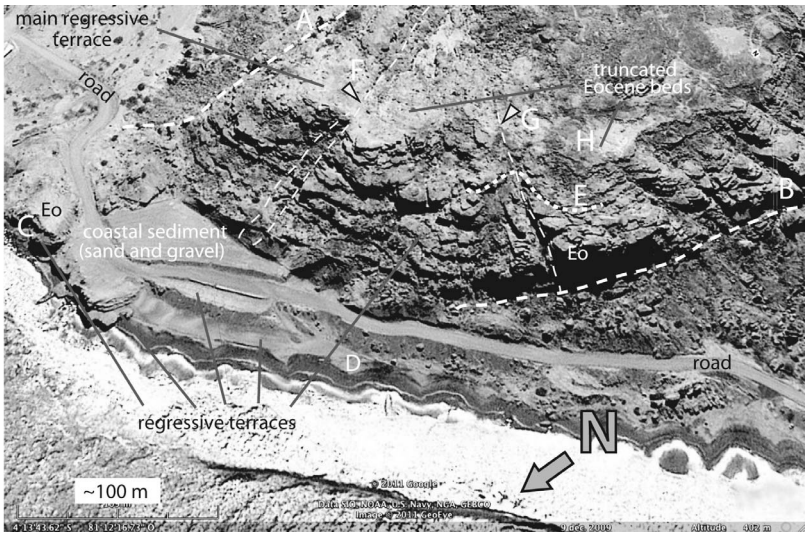

Figure 1. Staircase morphogenic landforms investigated along the Cabo Blanco transect (north of El Alto) in the original paper by *Bourgois et al.* [2007]. Note that: (1) Two normal faults [thick dash line, points A and B] bound the studied area to the east and to the west. The Eocene sandstones outcrop along a horst structure assumed to be older than the Taime Formation (i.e., older than 160 ± 12 ka [*Bourgois et al.*, 2007, Figure 8]). (2) The staircase signature of the Eocene sandstones extends seaward to the Present coastline, north of the road following the coastline. At point C, Eocene sandstone exhibits two regressive terraces at ~3 and 8.2 m above mean sea level. (3) These two specific regressive terraces extend 300–500 m to the southwest, following the coastline to point D. Between points C and D the terraces notch "Recent" coastal sediment. The regressive terraces, identified in the Eocene sandstone and "Recent" coastal sediment are coeval originating from similar erosion processes. (4) Faults (thin dash line) assumed to be older than the Taime Formation cut across the Eocene sandstones. Although no bed-to-bed link of Eocene sandstone bedding is possible along these faults the regressive terrace and associated cliff connect from one side to the other side of the faults as exemplified along the dotted line (point E). (5) Along the main regressive terrace, the pre-Taime faults (thin dashed line) exhibit no morphologic expression (at points F and G). At point H the Eocene sandstone bedding shows upward truncation (i.e., the regressive terrace dipping 5–8° seaward truncate the Eocene sandstone bedding, which dips 10° landward). These five lines of evidence added to those reported in the original paper [*Bourgois et al.*, 2007] document that no erosion process other than that originating from breaking wave abrasion is realistic. Eo, Eocene sandstone. Screenshot from 2007 Google Earth™, imagery© Google Inc. available at http://earth.google.com/intl/fr/download-earth.html, used with permission.

both in space and time with a recurrence time of about 10 days. Following *Horel and Cornejo Garrido* [1986] and *Goldberg et al.* [1987], *Takahashi* [2004] suggests that the thermally driven sea breeze circulation, which brings low-level moist air inland, and helps it rise up the western slope of the Andes inducing the extreme rainfall event. In other words, a minimum elevation of the moist air is needed for the genesis of intense convective events. It suggests that the coastal strip is not prone to such extreme rainfall events. A recent paper [*Douglas et al.*, 2009]

Table 1. The ^{10}Be Concentrations and Ages Revised Considering the Updated ^{10}Be Half-Life

Sample	Latitude (°S)	Longitude (°W)	Altitude (m)	Depth (cm)	Spallation[a] (at/g/yr)	Slow Muons[a] (at/g/yr)	Fast Muons[a] (at/g/yr)	^{10}Be (at/g)	Tmin (ka)
N02	4°13.98	81°10.57	296	0–5	3.78	0.0135	0.0457	212,659 ± 21,526	71.1 ± 7.2
N01*	4°13.98	81°10.57	293	700	3.79	0.0135	0.0456	57,130 ± 16,581	
N03	4°19.93	81°00.53	342	0–5	3.92	0.0138	0.0467	41,606 ± 9387	n.a.
N04*	4°19.92	81°00.41	362	800	3.97	0.0139	0.0472	42,354 ± 29,975	n.a.
N05	4°13.73	81°12.23	50	0–5	3.16	0.0120	0.0406	21,846 ± 4703	9.1 ± 2
N07	4°13.85	81°12.28	94	0–5	3.26	0.0122	0.0415	70,769 ± 7256	23.6 ± 2.4
N06*	4°13.67	81°12.19	24	700	3.10	0.0118	0.0401	7,295 ± 1896	
N10	5°08.41	81°10.46	82	0–5	3.22	0.0122	0.0413	501,644 ± 35,768	159.3 ± 11.4
N11*	5°08.73	81°10.41	0	0–5	3.03	0.0117	0.0397	18,241 ± 4115	
N12	5°48.48	81°03.12	116	0–5	3.30	0.0124	0.0419	615,952 ± 35,595	198.9 ± 11.5
N13*	5°48.26	81°02.95	10	1000	3.04	0.0117	0.0399	21,352 ± 4940	

[a]Surface production; n.a., not applicable.

documents that, in general terms, the mean precipitation during the period January–April 1998 the El Niño event is similar in spatial structure to that shown for the 1982–1983 event. The extreme rainfall is close to the base of the Andes on the Pacific slope, with much smaller quantities along the coastal strip. Also, the greatest enhancement of rainfall on wet days is found around the Piura/Chulucanas area. The analyses of rain gauge observations for January–April 1998 document that less than 10 mm.day^{-1} of rainfall occurred along the coastal strip of northern Peru located between 4 and 6°S (i.e., from north of Cabo Blanco to Sechura, including the area studied in 2007). However, it should be noted that no rain gauge station exists in the Cabo Blanco studied area. The nearest station (i.e., the Pananga station) is located 65–70 km to the ESE, east of the Amotapes massif divide. The coastal area studied by *Bourgois et al.* [2007], extending less than 3–4 km from the coastline, is located along the driest strip that characterizes the coastline from 4 to 6°S, including during the El Niño events. The focal point of extreme rainfall being located at more than 160 km southeast of the studied area (i.e., east of the Amotapes divide) substantiates what was stated in the original paper by *Bourgois et al.* [2007]. The landforms dated using the in situ produced ^{10}Be cosmonuclide have suffered very little erosion since exposure.

4. The ^{10}Be Analyses

[4] As evidenced in the maps and figures of *Bourgois et al.* [2007], surface boulders are not affected by topographic shielding because they lie on flat surfaces. Therefore the shielding factor used for these samples is 1. For reference samples shielded by the block itself, the shielding factor is the same as the one used for the top surface, but the productions were corrected for depth.

[5] The equation used by *Bourgois et al.* [2007] was

$$C_{(x,\varepsilon,t)} = \frac{P_n}{\frac{\varepsilon}{\Lambda_n}+\lambda}.e^{-\frac{x}{\Lambda_n}}\left[1-e-t\left(\frac{\varepsilon}{\Lambda_n}+\lambda\right)\right] + \frac{P_{\mu s}}{\frac{\varepsilon}{\Lambda_{\mu s}}+\lambda}.e^{-\frac{x}{\Lambda_{\mu s}}}\left[1-e-t\left(\frac{\varepsilon}{\Lambda_{\mu s}}+\lambda\right)\right] + \frac{P_{\mu f}}{\frac{\varepsilon}{\Lambda_{\mu f}}+\lambda}.e^{-x\Lambda_{\mu f}}\left[1-e-t\left(\frac{\varepsilon}{\Lambda_{\mu f}}+\lambda\right)\right] - C_0.e^{-\lambda t}$$

where C(x, ε, t) is the ^{10}Be concentration as a function of depth x (g/cm^2), ε is the erosion rate (g/cm^2/yr) and t is the exposure time (yr); C_0 is the maximum ^{10}Be concentration that might have been present when exposure at the surface started; this concentration is given by reference sample (This approach is not applicable for samples N03 and N04 because the exposure time after deposition was most likely not long enough to allow sample N03 to accumulate more ^{10}Be than its reference sample N04); Λ_n, $\Lambda\mu_s$, and $\Lambda\mu_f$ are the effective apparent attenuation lengths (g/cm^2), for neutrons, slow muons, and fast muons, respectively. P_n, $P\mu_s$, and $P\mu_f$ are the ^{10}Be production rate for spallation, slow and fast muons respectively. All calculations were performed using attenuation lengths of 150, 1500, and 5300 g/cm^2 with associated relative contributions to the total surface production rate of 1.50%, and 0.65% for slow muons and fast muons, respectively. These values are based on field-calibrated measurements [*Braucher et al.*, 2003]. The sea level high latitude spallation production of 5.1 at/g/yr rate was scaled to the altitude and latitude of samples [*Lal*, 1991]. However, since 2007, several physical parameters have been reevaluated (^{10}Be half live, spallation and muon production rates). Table 1 presents the updated results using the revised ^{10}Be half-life of (1.387 ± 0.012) Ma [*Korschinek et al.*, 2010; *Chmeleff et al.*, 2010], a modern ^{10}Be spallation production rate at sea level and high latitude of 4.5 ± 0.3 atoms/g/a, and the muon scheme of *Braucher et al.* [2011]. Revised ^{10}Be concentrations arise from the normalization to NIST SRM 4325 standard whose ratio has been remeasured by *Nishiizumi et al.* [2007]. The revised exposure ages that are 12 to 21% higher than those previously published are minimum exposure ages considering that negligible denudation rate is assumed (see references in the original paper).

5. Shoreline Angle Concept

[6] Although being against the uniformitarianism fundamental principle [*Hutton*, 1788; *Lyell*, 1830], it is commonly accepted that Pleistocene and Holocene strandlines have formed through different processes along active margin [*Lajoie*, 1986; *Lajoie et al.*, 1991; *Anderson et al.*, 1999; *Pedoja et al.*, 2011]. Because the sea level rise has not fluctuated significantly during the past 5–7 kyr, *Lajoie* [1986] assumed that uplifted Holocene strandlines do not represent an eustatic signature but rather episodic crustal movements identical to historical strandlines produced by abrupt coseismic uplift [*Lajoie et al.*, 1991; *Chappell et al.*, 1996; *Ota and Yamaguchi*, 2004]. Along rapidly uplifting forearc areas such as Japan, Alaska, Taiwan, and New Zealand, geomorphic analyses documents uplift elevation of strandlines ranging from less than a meter to 9–16 m following a 0.5 to 1.7 kyr approximate earthquake recurrence. At these areas, calculated uplift rates range from ~1 to 15 mm.yr^{-1} for the past 5–6 kyr.

[7] Conversely, a flight of emergent Pleistocene strandlines, older than 5–7 ka is proposed to be the geologic record of periodic glacioeustatic sea level highstands superimposed on a steadily rising coastline [*Lajoie*, 1986; *Lajoie et al.*, 1991]. In the field, the so-called shoreline angle (i.e., paleostrandline) records age and elevation signatures of a specific highstand. In this model, brief sea level highstands are successively recorded [*Bloom et al.*, 1974; *Chappell and Shackleton*, 1986] and most of strandlines formed during sea level lowstands are destroyed by subsequent sea level fluctuations. The well-documented records of emergent coral reef strandlines along the Huon Peninsula of Papua New Guinea [*Veeh and Chappell*, 1970] provided evidence for the model proposed by *Lajoie* [1986] to work. Also, it allowed a paleo–sea level curve reconstruction back to ~340 ka ago [*Bloom et al.*, 1974; *Chappell and Shackleton*, 1986; *Linsley*, 1996]. However, in order to disentangle the tectonic and eustatic signals at Huon peninsula, *Chappell et al.* [1996] have hypothesized similar average Holocene and late Pleistocene uplift rates.

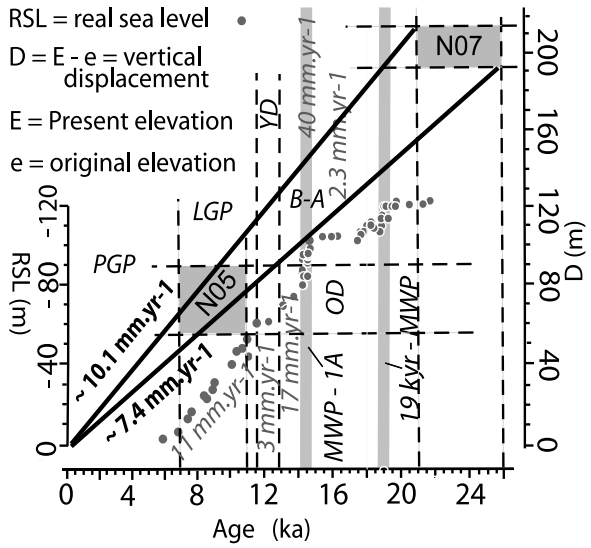

Figure 2. Uplift rate reconstruction (thick black lines). During the past 21.2–26 kyr, the Cabo Blanco segment uplifted at rates between ~7.4 and 10.1 mm.yr^{-1} (bold number). The net vertical crustal displacement (D) is the difference between the Present elevation (E) and the original elevation (e) of a strandline. It is the product of the strandline age (A) and the average displacement rate (R). (R) = D/A = (E − e)/A. The dark gray areas show (A) and (D) ±2 sigma for samples N05 and N07 collected at cliffs 9 and 16 [*Bourgois et al.*, 2007, Figure 9], respectively. Black dots show the sea level record spanning the last deglaciation [*Bard et al.*, 2010; *Gallup et al.*, 2002; *Fleming et al.*, 1998; *Imbrie et al.*, 1984; *Mesolella et al.*, 1969]. Also shown are average rates of sea level rise (italic numbers) for the periods 19 to 14.6 ka; 14.6 to 14.1 ka (MWP-1A); 14.1 to 12.9 ka; 12.9 to 11.6 ka and 11.6 to 6 ka [*Weaver et al.*, 2003]. B-A, Bølling-Allerød warm interval; LGP, Late Glacial Period (6–7 to 11.5 ka); MWP-1A, Meltwater pulse 1-A; 19 ka-MWP, Meltwater pulse at 19 ka; PGP, Post Glacial Period; YD, Younger Dryas cold event.

[8] Subsequently, the distinct and specific assumptions regarding Pleistocene strandlines and associated wave cut platforms have been considered as evidence for an implicit rule, but applied with no forethought. Hazardous along-strike correlations, both in space and time were proposed, including along the extremely active Andean forearc [*Ortlieb et al.*, 1996; *Cantalamessa and Di Celma*, 2004; *Saillard et al.*, 2009]. Poor age resolution of Pleistocene terraces based on chronostratigraphical correlation to sea level highstands resulted in major gaps between Holocene and Pleistocene average uplift rates, the latter being generally lower (i.e., lower than 1.5 mm.yr^{-1}) by an order of magnitude. Indeed, uplift rates ranging from 0.12 to 0.20 mm.yr^{-1} were reported along the coastal area of northern Peru [*DeVries*, 1988; *Macharé and Ortlieb*, 1994; *Pedoja et al.*, 2006] for the past 500–3000 kyr.

[9] Along the Cabo Blanco transect, three of the basic requirements for the shoreline angle model to work are unfulfilled. (1) The Cabo Blanco segment uplifted during the last deglaciation at a rate ranging from 7.4 to 10.1 mm yr^{-1} (Figure 2), significantly greater than the mean eustatic sea level rise during the Late Glacial Period (LGP) that makes it possible for lowstand coastal landforms to be preserved from destruction by reoccupation. (2) Reoccupation of the major wave cut platform (i.e., the Mancora Tablazo) occurring at 71.1 ± 7.2 ka (Figure 3) makes the chronostratigraphical correlations between terraces and highstands and the associated concept of shoreline angle useless. (3) Uplift occurred through a short-lived (~26 kyr) change in the tectonic deformation rate (see section 5). If the average tectonic uplift rate is higher than the mean sea level rise, the analysis using the so-called shoreline angle concept must be supplemented by detailed evolution of the subsequent/subcoeval coastal regressive terraces, and cautious age resolution. Whether wave cut platforms along separated segments such as those of northwestern Peru [*Bourgois et al.*, 2007] exhibit no along strike connection, no simple correlation from one segment to the other is possible. No extrapolation of uplift rates from

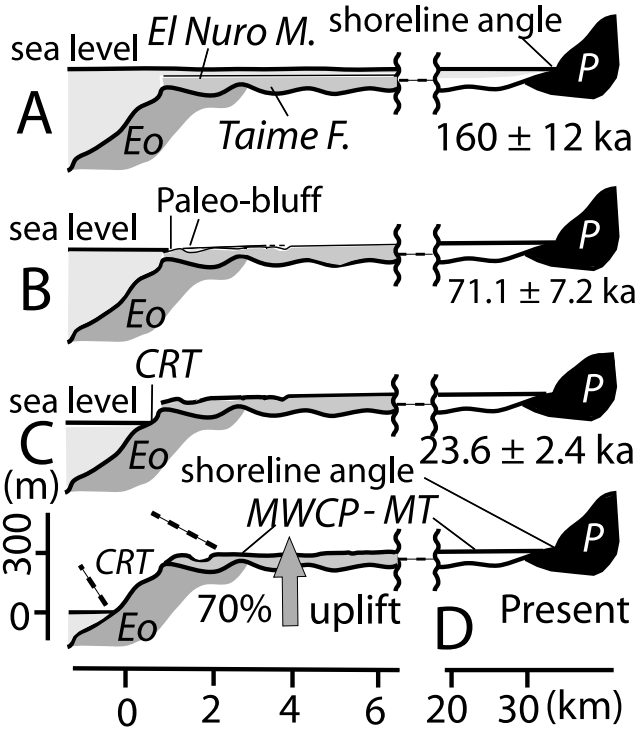

Figure 3. Tectonic evolution of the Cabo Blanco transect for the past 160 ± 12 kyr. (a) The shallow water El Nuro Member (Taime Formation) accumulated at 160 ± 12 ka. First emergence (not shown) of the Mancora Tablazo occurred probably during the Marine Isotope Stage 6 lowstand. (b) Reoccupation of the Mancora Tablazo occurred at 71.1 ± 7.2 ka. (c) The Mancora Tablazo was above sea level at 23.6 ± 2.4 ka. (d) Relationship between coastal regressive terraces and the major wave cut platform (i.e., the Mancora Tablazo) at Present. Note that no fault exists between these two different coastal landforms. The cross section between dashed lines is shown in the original paper by *Bourgois et al.* [2007, Figure 9a]. The arrow shows that major uplift of this area occurred after 23.6 ± 2.4 ka. CRT, Coastal regressive terrace; Eo, Eocene; MT, Mancora Tablazo; MWCP-MT, major wave cut platform (i.e., the Mancora Tablazo); P, Paleozoic (Amotapes massif).

segment to segment is possible. The tectonic history of each unconnected segment must be independently reconstructed [*Melnick et al.*, 2009]. If no along strike tie between terraces exists, no correlation should be done without age control.

[10] Along fast uplifting forearc areas, such as the northern Peru Andes along the Cabo Blanco segment, the shoreline angle model must be applied carefully, after a comprehensive investigation of the uplift rates. The analytical method developed in the field from the pioneering work of *Lajoie* [1986] must be rethought, with the shoreline angle concept being of secondary relevance in order to disentangle the complex history of coastal landform emergence. As a result, most of the sites previously studied along the Andean forearc must be checked using more careful field analysis [*Bourgois*, 2010] for process-oriented investigations as it was recently documented along the Costa Rican forearc segment [*Sak et al.*, 2009]. If applied to areas undergoing moderate tectonic deformation (i.e., mean sea level rise is greater than the average tectonic uplift rate), and previously carved wave cut platforms are not reoccupied, then the shoreline angle model remains relevant.

6. Mancora Tablazo Uplift Rate

[11] Along the Cabo Blanco segment [*Bourgois et al.*, 2007], the emergence (100–140 m) of the Mancora Tablazo occurred during the eustatic sea level fall of Marine Isotope Stage 3 and 2 (from 71.1 ± 7.2 to 23.6 ± 2.4 ka), in association with a very low uplift rate of less than 1 mm.yr^{-1}. In situ produced ^{10}Be cosmonuclide allowed dating of the exposure of coastal regressive terraces [*Bourgois et al.*, 2007, Figures 1, 3d, 5a, 5b, 9a and 9b] (Figure 1) located west of the Mancora Tablazo. Since the Mancora Tablazo and the coastal area evolved coevally, and remained tectonically coupled through time (Figure 3), the coastal regressive terraces recorded the tectonic history of the inboard major wave cut platform (i.e., the Mancora Tablazo) for the past 21.2–26 kyr. The Mancora Tablazo uplifted 204 ± 10 m during the last eustatic sea level rise (the past 19–23 ka). At 23.6 ± 2.4 ka began a major sequence of great earthquakes inducing an average uplift rate (Figure 2) ranging from 7.4 to 10.1 mm.yr^{-1} (Figure 2), making the shoreline angle model irrelevant.

[12] In northern Peru, regressive terraces of Holocene and Pleistocene age have the same coseismic origin suggesting similar relationship to the seismogenic zone at depth. In order to make comparison with other active coastal regions, a linear distribution of uplift through time was assumed for the past 160–200 kyr. This led to uplift rates ranging from 1.5 to 1.8 and 0.5 to 1.2 mm.yr^{-1}, for the Cabo Blanco segment. These rates are similar to those estimated elsewhere along the Andean forearc. The 6 to 10 times higher uplift rates at northern Peru result from accurate calculation of tectonic step duration. To hypothesize steadily rising coastlines through long lasting stable uplift rate, i.e., during 100–400 kyr or more, is inconsistent with the Peru forearc data. A long sequence of major earthquakes (coseismic uplift from 3 to 9 m) occurred during the past 21.2–26 kyr with a recurrence interval of about 800–1000 yr. The meter scale uplift and average recurrence interval of these earthquakes resemble those affecting the Huon peninsula during the so-called infrequent earthquakes [*Chappell et al.*, 1996] with ~1000–1200 yr recurrence intervals.

7. Conclusion

[13] After careful consideration of the points raised by *Pedoja et al.* [2011] we maintain the explanation proposed by *Bourgois et al.* [2007] for the evolution of the northwestern coastal plain of Peru, and tablazos. Along the Andes forearc [*Bourgois*, 2010], we reject the conjectures as based, uncritically, on the long-standing dogma of the shoreline angle concept.

[14] **Acknowledgments.** This work together with the initial paper by *Bourgois et al.* [2007] were funded by the Université Pierre et Marie Curie (UPMC) and the Centre National de la Recherche Scientifique (CNRS). We thank Tom Parsons for his thorough and constructive review.

References

Anderson, R. S., A. L. Densmore, and M. A. Ellis (1999), The generation and degradation of marine terraces, *Basin Res.*, *11*, 7–19, doi:10.1046/j.1365-2117.1999.00085.x.

Bard, E., B. Hamelin, and D. Delanghe-Sabatier (2010), Deglacial meltwater pulse 1B and younger dryas sea levels revisited with boreholes at Tahiti, *Science*, *327*, 1235–1237, doi:10.1126/science.1180557.

Bloom, A. L., W. S. Broecker, J. M. Chappell, R. K. Matthews, and K. J. Mesolella (1974), Quaternary sea level fluctuations on a tectonic coast: New 230Th/234U dates from the Huon peninsula, New Guinea, *Quat. Res.*, *4*, 185–205, doi:10.1016/0033-5894(74)90007-6.

Bourgois, J. (2010), A comment on "Non-steady long-term uplift rates and Pleistocene marine terrace development along the Andean margin of Chile (31°S) inferred from 10Be dating", *Earth Planet. Sci. Lett.*, *296*, 502–505, doi:10.1016/j.epsl.2010.05.018.

Bourgois, J., F. Bigot-Cormier, D. Bourles, R. Braucher, O. Dauteuil, C. Witt, and F. Michaud (2007), Tectonic records of strain buildup and abrupt coseismic stress release across the northwestern Peru coastal plain, and continental slope during the past 200 kyr, *J. Geophys. Res.*, *112*, B04104, doi:10.1029/2006JB004491.

Braucher, R., E. T. Brown, D. L. Bourlès, and F. Colin (2003), In situ-produced ^{10}Be measurements at great depths: Implications for production rates by fast muons., *Earth Planet. Sci. Lett.*, *211*, 251–258, doi:10.1016/S0012-821X(03)00205-X.

Braucher, R., S. Merchel, J. Borgomano, and D. L. Bourlès (2011), Production of cosmogenic radionuclides at great depth: A multi element approach, *Earth Planet. Sci. Lett.*, *309*, 1–9, doi:10.1016/j.epsl.2011.06.036.

Cantalamessa, G., and C. Di Celma (2004), Origin and chronology of Pleistocene marine terraces of Isla de la Plata and of flat, gently dipping surfaces of the southern coast of Cabo San Lorenzo (Manabi, Ecuador), *J. South Am. Earth Sci.*, *16*, 633–648, doi:10.1016/j.jsames.2003.12.007.

Carranza, L. (1891), Contracorriente maritima observada en Payta y Pacasmayo, *Bol. Soc. Geogr. Lima*, *1*, 344–345.

Chappell, J., and N. J. Shackleton (1986), Oxygen isotopes and sea level, *Nature*, *324*, 137–140, doi:10.1038/324137a0.

Chappell, J., Y. Ota, and K. Berrymann (1996), Late Quaternary coseismic uplift history of Huon peninsula, Papua New Guinea, *Quat. Sci. Rev.*, *15*, 7–22, doi:10.1016/0277-3791(95)00062-3.

Chmeleff, J., F. von Blackenburg, K. Kossert, and D. Jackob (2010), Determination of the ^{10}Be half-life by multicollector ICP-MS and liquid scintillation counting, *Nucl. Instrum. Methods Phys. Res., Sect. B*, *268*, 192–199, doi:10.1016/j.nimb.2009.09.012.

DeVries, T. J. (1988), The geology of late Cenozoic marine terraces (tablazos) in northwestern Peru, *J. South Am. Earth Sci.*, *1*, 121–136, doi:10.1016/0895-9811(88)90030-2.

Douglas, M. W., J. Mejia, N. Ordinola, and J. Boustead (2009), Synoptic variability of rainfall and cloudiness along the coasts of northern Peru and Ecuador during the 1997/98 El Niño event, *Mon. Weather Rev.*, *137*, 116–136, doi:10.1175/2008MWR2191.1.

Eguiguren, D. V. (1894), Las Lluvias de Piura, *Bol. Soc. Geogr. Lima*, *4*, 241–258.

Fleming, K., P. Johnston, D. Zwart, Y. Yokoyama, K. Lambeck, and J. Chappell (1998), Refining the eustatic sea-level curve since the Last Glacial Maximum using far- and intermediate-field sites, *Earth Planet. Sci. Lett.*, *163*, 327–342, doi:10.1016/S0012-821X(98)00198-8.

Gallup, C. D., H. Cheng, F. W. Taylor, and R. L. Edwards (2002), Direct determination of the timing of sea level change during Termination II, *Science*, *295*, 310–313, doi:10.1126/science.1065494.

Goldberg, R. A., G. Tisnado, and R. A. Scofield (1987), Characteristics of extreme rainfall events in northwestern Peru during the 1982–1983 El Niño period, *J. Geophys. Res.*, *92*, 14,225–14,241, doi:10.1029/JC092iC13p14225.

Horel, J. D., and A. G. Cornejo-Garrido (1986), Convection along the coast of northern Peru during 1983: Spatial and temporal variation of clouds and rainfall, *Mon. Weather Rev.*, *114*, 2091–2105, doi:10.1175/1520-0493(1986)114<2091:CATCON>2.0.CO;2.

Hutton, J. (1788), The theory of the Earth; or an investigation of the laws observable in the composition, dissolution, and restoration of land upon the Globe, *Trans. R. Soc. Edinburg.*, *1*, 209–304.

Imbrie, J., J. D. Hays, D. G. Martison, A. McIntyre, A. C. Mix, J. J. Morley, N. G. Pisias, W. L. Prell, and N. J. Shackleton (1984), The orbital theory of Pleistocene climate: Support from a revised chronology of the marine d^{18}O record, in *Milankovitch and Climate*, *NATO ASI Ser.*, part 1, edited by A. L. Berger, pp. 269–305, Springer, New York.

Korschinek, G., et al. (2010), A new value for the ^{10}Be half-life by heavy-ion elastic recoil detection and liquid scintillation counting, *Nucl. Instrum. Methods Phys. Res., Sect. B*, *268*, 187–191, doi:10.1016/j.nimb.2009.09.020.

Lajoie, K. R. (1986), Coastal tectonics, in *Active Tectonics*, pp. 95–124, Natl. Acad., Washington, D. C.

Lajoie, K. R., D. J. Ponti, C. L. I. Powell, S. A. Mathieson, and A. M. Sarna-Wojcicki (1991), Emergent marine strandlines and associated sediments, coastal California: A record of Quaternary sea level fluctuations, vertical tectonic movements, climatic changes, and coastal processes, in *Quaternary Nonglacial Geology: Conterminous U.S.*, *Geology of North America*, edited by R. B. Morrison, pp. 190–203, Geol. Soc. Am., Boulder, Colo.

Lal, D. (1991), Cosmic ray labeling of erosion surfaces: In situ nuclide production rates and erosion models, *Earth Planet. Sci. Lett.*, *104*, 424–439, doi:10.1016/0012-821X(91)90220-C.

Linsley, B. K. (1996), Oxygen-isotope record of sea level climate variations in the Sulu Sea over the past 150,000 years, *Nature*, *380*, 234–237, doi:10.1038/380234a0.

Lyell, C. (1830), *Principles of Geology: Being an Attempt to Explain the Former Changes of the Earth's Surface, by Reference to Causes Now in Operation*, vol. 1, 481 pp., John Murray, London.

Macharé, J., and L. Ortlieb (1994), Morfoestratigrafia de los tablazos del noroeste Peruano: Neotectonica y fluctuaciones del nivel del mar, paper presented at VIII Congreso Peruano de Geologia, Soc. Geol. del Perú, Lima.

Melnick, D., B. Bookhagen, M. R. Strecker, and H. P. Echtler (2009), Segmentation of megathrust rupture zones from fore-arc deformation patterns over hundreds to millions years, Arauco peninsula, Chile, *J. Geophys. Res.*, *114*, B01407, doi:10.1029/2008JB005788.

Mesolella, K. J., R. K. Matthews, W. S. Broecker, and D. L. Thurber (1969), The astronomical theory of climatic change: Barbados data, *J. Geol.*, *77*, 250–274, doi:10.1086/627434.

Nishiizumi, K., M. Imamura, M. W. Caffe, J. R. Southon, R. C. Finkel, and J. McAninch (2007), Absolute calibration of ^{10}Be AMS standards, *Nucl. Instrum. Methods Phys. Res., Sect. B*, *58*, 403–413.

Ortlieb, L., S. Barrientos, and N. Guzman (1996), Co-seismic coastal uplift and coralline algae record in northern Chile: The 1995 Antofagasta earthquake case, *Quat. Sci. Rev.*, *15*, 949–960, doi:10.1016/S0277-3791(96)00056-X.

Ota, Y., and M. Yamaguchi (2004), Holocene coastal uplift in the western Pacific Rim in the context of late Quaternary uplift, *Quat. Int.*, *120*, 105–117, doi:10.1016/j.quaint.2004.01.010.

Pedoja, K., L. Ortlieb, J. F. Dumont, J. F. Lamothe, B. Ghaleb, M. Auclair, and B. Labrousse (2006), Quaternary coastal uplift along the Talara arc (Ecuador, northern Peru) from new marine terrace data, *Mar. Geol.*, *228*, 73–91, doi:10.1016/j.margeo.2006.01.004.

Pedoja, K., L. Ortlieb, T. J. DeVries, J. Machare, L. Audin, and V. Regard (2011), Comment on "Tectonic record of strain build-up and abrupt coseismic stress release across the northwestern Peru coastal plain, shelf, and continental slope during the past 200 kyr" by Jacques Bourgois et al., *J. Geophys. Res.*, doi:10.1029/2011JB008321, in press.

Plafker, G. (1969), Tectonics of the March 27, 1964, Alaska earthquake, *U.S. Geol. Surv. Prof. Pap.*, *543*, 74 pp.

Saillard, M., S. R. Hall, L. Audin, D. L. Farber, G. Hérail, J. Martinod, V. Regard, R. C. Finkel, and F. Bondoux (2009), Non-steady long-term uplift rates and Pleistocene marine terrace development along the Andean margin of Chile (31°S) inferred from ^{10}Be dating, *Earth Planet. Sci. Lett.*, *277*, 50–63, doi:10.1016/j.epsl.2008.09.039.

Sak, P. B., D. M. Fisher, T. W. Gardner, J. S. Marshall, and P. C. LaFemina (2009), Rough crust subduction, forearc kinematics, and Quaternary uplift rates, Costa Rican segment of the Middle America trench, *Geol. Soc. Am. Bull.*, *121*, 992–1012, doi:10.1130/B26237.1.

Spruce, R. (1864), *Notes on the Valleys of Piura and Chira in Northern Peru and on the Cultivation of Cotton Therein*, 81 pp., Eyre and Spottswoodie, London.

Sunamura, T. (1992), *Geomorphology of Rocky Coasts*, edited by E. C. F. Bird, John Wiley, Hoboken, N. J.

Takahashi, K. (2004), The atmospheric circulation associated with extreme rainfall events in Piura, Peru, during the 1997–1998 and 2002 El Niño events, *Ann. Geophys.*, *22*, 3917–3926, doi:10.5194/angeo-22-3917-2004.

Thatcher, W. (1984), The earthquake deformation cycle at the Nankai trough, southwest Japan, *J. Geophys. Res.*, *89*, 3087–3101, doi:10.1029/JB089iB05p03087.

Veeh, H. H., and J. Chappell (1970), Astronomical theory of climatic change: Support from New Guinea, *Science*, *167*, 862–865, doi:10.1126/science.167.3919.862.

Weaver, A. J., O. A. Saenko, P. U. Clark, and J. X. Mitrovica (2003), Meltwater pulse 1A from Antarctica as a trigger of the Bølling-Allerød warm interval, *Science*, *299*, 1709–1713, doi:10.1126/science.1081002.

J. Bourgois, Institut des Sciences de la Terre, UMR 7193, CNRS, Université Pierre et Marie Curie, Case Courrier 124, 4 place Jussieu, F-75252 Paris, CEDEX 05, France.

D. Bourles and R. Braucher, Centre Européen de Recherche et d'Enseignement des Geosciences de l'Environnement, UMR 6635, Europôle Méditerranéen de l'Arbois, Aix-Marseille Université, F-13545 Aix-en-Provence, CEDEX 04, France.